Internal calibration of the LUX detector using tritiated methane

LUX Collab List

September 24, 2013

Abstract

We have developed a new method to inject tritiated methane into detectors which utilize liquid and gas phase noble gases as an internal calibration source. The ability to use internal calibration sources is critical in large scale particle physics experiments. Our system uses volume sharing techniques to inject a finely tuned amount of tritiated methane into the detector, and uses a zirconium getter to remove the tritiated methane after the calibration has been completed. We present data from the LUX detector to prove our tritiated methane system can calibrate electron recoil events and remove the internal source to undetectable levels afterward.

I. Introduction

The Large Underground Xenon detector (LUX) is a dual phase time projection chamber containing 350 kg of xenon used as the target mass for WIMP detection. The xenon is cooled by a thermosyphon system until it condenses in the detector. Recoil events in the detector will produce a scintillation signal (referred to as S1) and ionization. Photo-multiplier tubes can be used to measure the scintillation light, while the ionization can be drifted to an anode located in the gas phase of the detector. Once the charged particles are accelerating toward the anode in the xenon gas they will create a secondary scintillation signal (referred to as S2). Nuclear recoil events have higher ionization density, leading to a higher recombination probability, resulting in a higher S1 yield and lower S2 yield than electron recoil events of the same energy. Thus, the different quenching factors can be used to distinguish the two types of events. The location of the S2 signal provides the x and y coordinates of the recoil event, while the time between the S1 and S2 signal provides the z coordinate of the recoil event. This allows the primary event to be localized within one centimeter in all three spacial dimensions. The

xenon space is shielded by a 300 ton water tank which houses additional photomultiplier tubes for cosmic ray vetoing [1, 2].

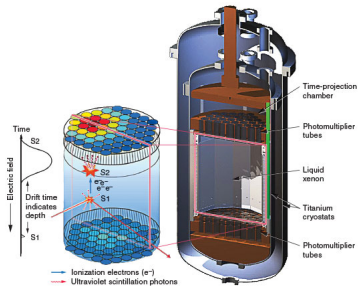

Figure 1: Image depicting the internals of the LUX detector.

In order to distinguish dark matter signals in the detector from background signals the detector's response to nuclear recoil events and electron recoil events must be well understood. For calibrating electron recoil events it is common to use an external beta emitter such as cesium-137. However, the xenon in LUX has a strong self-shielding characteristic at UV wavelengths. While this is convenient for eliminating background radiation, it creates a challenge for calibrating the innermost regions of a detector the size of LUX.

To overcome this problem the LUX collaboration is making use of internal calibration sources. An ideal internal calibration source would need to be a single beta emitter in the energy range of interest (< 15 keV) which can be dissolved into the liquid xenon in the detector. Furthermore, the source must be made of a material with low electronegativity so that it will not poison the detector's charge drift length. Similarly the source cannot attenuate the UV scintillation light produced by events in the detector. To achieve a reliable calibration in all regions of the detector the source would need to have a long enough life time to diffuse throughout the entire detector (a few hours). Finally, there must be a method for removing the source once the calibration has finished. This could simply mean waiting for the source to decay if its half life is short, or actively purifying the source out of the detector if its half life is long [3].

Tritium meets several of these requirements. It is a beta emitter with a Q-value of 18 keV that produces a broad spectrum over the entire energy range of interest. Its 12.3 year half life means that the source will have plenty of time to dissolve uniformly throughout the detector. However, this long half life is potentially dangerous, since one can not simply wait for it to decay away – it must be actively removed from the detector when the calibration is completed. To complicate this matter bare tritium sticks to most surfaces, including materials like teflon, polyethylene, and steel which make up the majority of most xenon detectors.

To make tritium removal more feasible we have made use of tritiated methane (CH_3T). Methane is highly inert due to its fully saturated carbon-hydrogen bonds. It has a diffusion constant in polyethylene that is 10 times smaller than hydrogen, and it does not capture elec-

trons that will be drifting through the detector. By replacing one of the hydrogen atoms in a methane molecule with tritium we combine the strength of both of these materials, resulting in the ideal internal calibration source.

II. Tritiated Methane Removal

To study the CH_3T removal efficiency of zirconium getters the University of Maryland built two separate systems to inject tritiated methane into a gaseous xenon and a liquid xenon environment. Both of these systems used zirconium getters to remove any CH_3T that was injected into them.

A. Gas Experiments

The gaseous xenon system consists of three sections. The first section, the xenon space, contains a xenon purifier which uses hot zirconium to remove the CH_3T, two xenon storage bottles used to move xenon through the system via cryopumping, and a proportional tube used to detect activity within the xenon space. The second section is a small transfer system which is used to inject consistent amounts of CH_3T into the xenon space with each injection. The final section consists of a CH_3T storage bottle used as the source of injections and a SAES MC1-905F methane purifier to remove unwanted contaminates prior to entering the xenon space.

The primary goal of this experiment

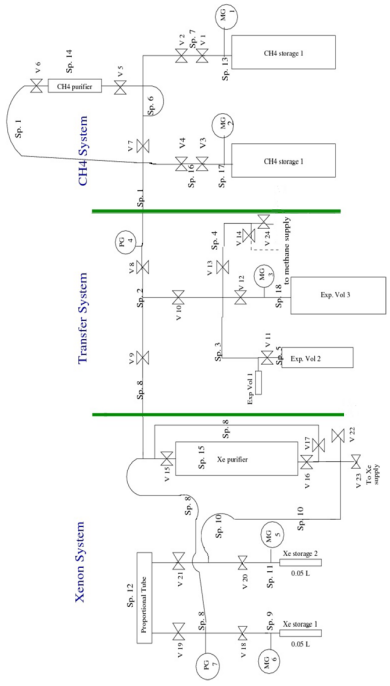

Figure 2: CH_3T gas system at UMD. Three sections of the system are distinguished with green lines. Circles labeled PG and MG are pressure gauges, and the hourglass shapes represent hand valves.

was to determine the purification efficiency and study residual contamination. There are two factors that dominate purification efficiency – flow rate through the purifier and rest time between subsequent purifications. High flow rates through the purifier can cool the zirconium inside, while inadequate rest time between purifications can lead to build up of methane on the surface of the zirconium beads. Both of these situations lead to a decrease in purifier efficiency.

The first black data point in Figure 3 is our worst purification efficiency, (96% +/- 1%) corresponding to our highest flow rate. (8 SLPM compared to the typical 0.3 SLPM) While we were unable to control the flow through our experiment as much as we desired, we are at least able to conclude that exceeding the maximum flow rate suggested for the purifier does significantly decrease purification efficiency.

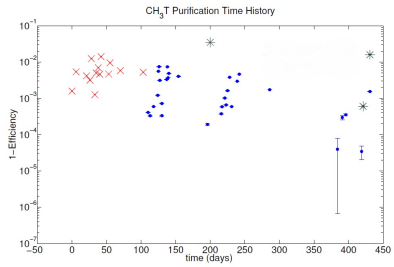

Figure 3: Single pass inefficiency of the purifier when removing CH_3T. The red and blue points indicate data taken by different students, while the black points indicate data for which the procedures were intentionally altered.

We found that allowing for ample rest time between purifications does significantly increase purification efficiency. Our best purifications were the first data points in each cluster in Figure 4. We were able to obtain efficiencies of 99.99% when the purifier was resting for three weeks or longer, and obtained efficiencies of 99% to 99.9% when the purifier was used on a daily basis.

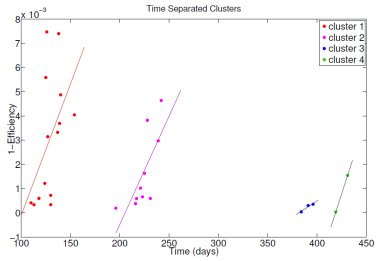

Figure 4: Time-separated clusters of purifications have an upward trend in purification inefficiency. Each cluster shown is separated in time by at least three weeks.

B. Liquid Experiments

We have also tested tritium removal from liquid xenon. Our liquid xenon system consists of two main sections, the CH_3T injection system and the liquid xenon system. We will first discuss the set up of the tritium injection system, pictured below.

The injection system begins at the CH_3T storage bottle. This bottle is double valved for safety reasons. As with the gaseous experiments, we have a SAES MC1-905F methane purifier in series with the storage bottle. Following

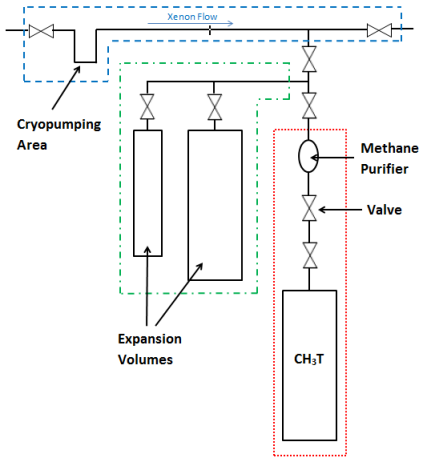

Figure 5: The tritium injection system for the liquid phase experiments at UMD. The red box indicates the CH_3T storage bottle and methane purifier area, the green box indicated the expansion volumes, and the box indicates the cryopumping and xenon flow through area.

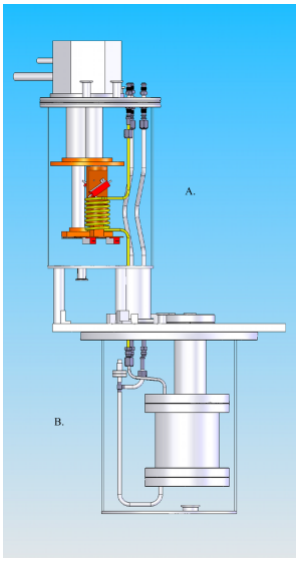

Figure 6: The liquid xenon system at UMD. (A) The xenon condenser consists of a helical coil cooled by a pulse tube refrigerator. (B) The liquid xenon storage vessel houses two PMTs to observe tritium decay.

the methane purifier there is a series of injection volumes branching off to the left. These injection volumes are designed to inject the desired amount of CH_3T into the xenon system. The last component of the injection system is located above the injection volumes. This plumbing is used to collect all of the CH_3T from the injection volume via cyropumping. After the plumbing has warmed, the xenon circulating outside of the injection system is rerouted through the cryopump plumbing to sweep all of the CH_3T into the xenon system.

The second section of our system, the liquid xenon system, is pictured below.

In the liquid xenon system, a pulse tube refrigerator cools a xenon gas condenser consisting of a helical coil of copper tubing. The condensed xenon then drips into a liquid xenon storage vessel. Inside of the liquid xenon storage vessel are two PMTs that face each other. These PMTs are used to observe xenon scintillation light from tritium decay. Once the vessel is filled both of these PMTs are submerged in the liquid xenon. Note that this means the system at UMD is a single phase detector, rather than a dual phase detector like LUX. Polyethylene or teflon curtains were installed in the inner cryostat to surround the PMTs

during some of our data sets. These curtains of plastic were used to study outgassing effects in our detector. It should be noted that in the plumbing leading to the liquid xenon system there is a SAES Zirconium getter (pcf4c3r1) used to purify the tritiated methane out of the system when desired.

During our liquid phase experiments, our experimental procedure consisted of taking an adequate amount of background data, injecting CH_3T into the liquid xenon, waiting for the CH_3T event rate to plateau, then purifying the CH_3T out of the xenon. During the data sets in which teflon or polyethylene curtains were installed around our PMTs we bypassed our purifier after initally purifying away the CH_3T so that outgassing effects could be studied. Injection activities for our liquid phase experiment ranged from 1487 ± 35.06 Bq to 12164 ± 1028.11 Bq.

A detailed list of our purification efficiency measurements in liquid xenon is included in Table 1. Note that the rise in background rate during our polyethylene runs is due to a change in PMT gain. Using the lessons learned from the gaseous xenon experiments we were able to achieve an average purification efficiency of 99.999% in our liquid experiments, where we define our purification efficiency to be

$$\text{Purification Efficiency} = 1 - \frac{A-B}{I-B},$$

where A is the background event rate after injecting CH_3T, B is the background event rate prior to injecting CH_3T, and I is the injected CH_3T activity as observed by out PMTs. We find that the addition of plastic curtains around our PMTs does not impair our ability to remove CH_3T at $> 99.998\%$ levels. To illustrate the effectiveness of CH_3T removal, an overlay of injected and purified CH_3T spectra is included in Figure 7.

Observed Injection Activity (Bq)	Background Before Injection (Bq)	Background After Injection (Bq)	Purification Efficiency	Type of Plastic
10415 ± 140	4.78 ± 0.38	4.99 ± 0.39	0.99998 ± 0.000054	No Plastic
3295 ± 46	4.99 ± 0.39	5.01 ± 0.39	0.99999 ± 0.00017	No Plastic
2836 ± 22	5.01 ± 0.39	4.76 ± 0.39	1.00009 ± 0.00020	No Plastic
12164 ± 1028	4.72 ± 0.39	5.09 ± 0.39	0.99997 ± 0.000082	No Plastic
11033 ± 1766	5.09 ± 0.39	4.69 ± 0.38	1.00004 ± 0.00015	No Plastic
9435 ± 180	3.74 ± 0.38	5.32 ± 0.39	0.99983 ± 0.000061	Stock Teflon
7666 ± 226	5.11 ± 0.39	5.23 ± 0.39	0.99998 ± 0.000082	Stock Teflon
6043 ± 446	5.23 ± 0.39	5.23 ± 0.39	1.00000 ± 0.00016	Stock Teflon
4504 ± 220	4.64 ± 0.39	4.71 ± 0.40	0.99998 ± 0.00016	No Plastic
1487 ± 35	5.79 ± 0.41	5.76 ± 0.41	1.00002 ± 0.00043	LUX Polyethylene

Table 1: CH_3T purification efficiencies in liquid xenon.

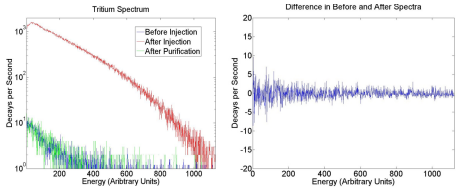

Figure 7: Left: Overlay of spectra seen by PMTs in the liquid xenon detector. The blue spectrum is what is seen by the PMTs prior to injecting tritium, the red spectrum is what is seen by the PMTs after injecting tritium, and the green spectrum is what is seen by the PMTs after purifying the xenon to remove any injected tritiated methane. Right: The difference between the before injection and after purification spectra.

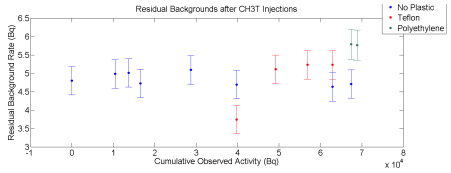

Figure 8: Residual background rates over time in our detector after purifying the CH_3T out of the xenon. Blue data points are data sets in which no plastic curtains where used inside of the detector, red data points are data sets in which teflon curtains where used inside of the detector, and green data points are data sets in which polyethylene curtains were used inside of the detector.

Cumulatively, we have injected over 68,000 observed becquerel of CH_3T into our liquid xenon. Although systematic errors lead to a fluctuation of our residual background rates, we see no upward trend in our data set as the cumulative observed injection activity rises.

III. Simulations

For an internal calibration of the LUX detector to be successful two conditions had to be met. First, there must be enough events detected during the calibration to accurately measure the tritium spectrum. We chose to define a factor of 100 over the number of background events which LUX collects over 300 days to be a sufficient number of CH_3T decays for the calibration. The nominal background rate of LUX is $8.4 \times 10^{-4} \frac{events}{keV*kg*day}$. Since the fiducial volume of LUX is 100 kg, and the energy spectrum of interest ranges from 1.3 keV to 8 keV, we expect 170 background events in LUX over 300 days. Thus, we set a goal of collecting around 17,000 events during our CH_3T calibration. The second condition for a successful CH_3T calibration is that any residual CH_3T remaining after purification must not add a significant contribution to the background rate in the detector. We chose to define the tolerable CH_3T activity after a calibration to be 5% of the nominal background rate in LUX, setting a limit on the residual CH_3T activity of $8.4 \times 10^{-4} \frac{events}{keV*kg*day} \times 100\ kg \times 6.7\ keV \times \frac{1\ day}{86400\ sec} \times 0.05 = 0.33 \mu Bq$.

To achieve these goals we had to determine how much initial CH_3T activity to inject into LUX by numerically modeling the purification and residual diffusion of CH_3T in LUX. Fick's two laws are simple

differential equations which describe the diffusion process. The first law describes the flux of a material through a surface. Its general form is given by

$$J = -D\nabla\phi,$$

where J is the amount of material per unit area per unit time, D is the diffusion coefficient, and ϕ is the concentration function of the material. Combining this with the continuity equation,

$$\frac{\delta\phi}{\delta t} + \nabla \cdot J = 0,$$

which states that a change in density in any part of the system is due to inflow and outflow of material results in Fick's second law,

$$\frac{\delta\phi}{\delta t} = D\nabla^2\phi,$$

which describes the transport of a material by diffusion.

To implement these diffusion laws into our model we must determine the diffusion coefficient of CH_3T in the plastics of LUX. At room temperature, the diffusion coefficient of methane in Teflon is measured to be $2.3 \times 10^{-7} \frac{cm^2}{sec}$. [4] The temperature dependence of this diffusion constant is modeled by the Arrhenius equation,

$$D = Ae^{\frac{-E_a}{RT}},$$

where E_a is the activation energy, R is the gas constant, and T is the temperature. This suggests an adjustment factor to the diffusion constant of 10^{-6} at liquid xenon temperature. This adjustment factor is equivalent to increasing the thickness of the plastic in our model by a factor of 1,000. For this reason we are motivated to use half-infinite line boundary conditions in our diffusion model.

The analytic solution to Fick's second law using half-infite line boundary conditions is

$$\phi(x,t) = KC_{out} - \int_0^t erf(\frac{x}{\sqrt{4D(t-\tau)}})KC_{out}^{\cdot}(\tau)d\tau - KC_{out}(0)erf(\frac{x}{\sqrt{4Dt}}),$$

where K is the solubility of the material and C_{out} is the outside concentration of the material. [5] For the outgassing process we are only interested in the flux of material out of the plastic. This is given by Fick's first law evaluated at $x = 0$,

$$J_{out}(t) = -K\sqrt{\frac{D}{\pi}}(\int_0^t \frac{C_{out}^{\cdot}(\tau)}{\sqrt{t-\tau}}d\tau + \frac{C_{out}(t)}{\sqrt{t}}),$$

where the sign has been flipped since the flux of material is outward. We see that it is no longer possible to evaluate K and D separately, since the diffusion in and out of the plastic is completely determined by the time-dependent concentration outside of the plastic. To simplify our model, we define a new constant

$$G = K\sqrt{\frac{D}{\pi}}.$$

A. Outgassing Experiments

To determine the value of G for our simulations we surrounded the PMTs in our liquid phase R&D experiment with

polyethylene or teflon panels during some of our data sets. The experimental procedure for these data sets was to collect an adequate amount of background data, inject CH_3T into the liquid xenon, wait for the CH_3T event rate to plateau, purify the CH_3T away until we reached the initial background event rate, then bypass the purifier on our system to study outgassing effects. Once the purifier had been bypassed we discovered two sources of residual CH_3T contamination.

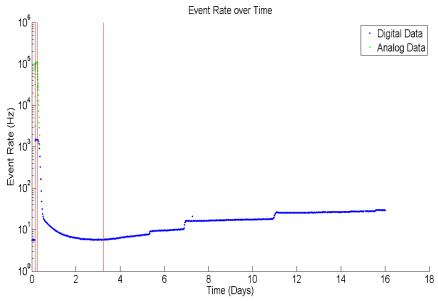

Figure 9: A time histogram of the CH_3T rate in our system. The third red line indicates when our purifier was bypassed.

We see a gradual rise in CH_3T activity after bypassing our purifier due to outgassing of CH_3T from the plastic panels. This outgassing effect will be discussed in detail in Section 4. In addition to this steady rise, we see large steps in CH_3T activity at random intervals. These step features occur every 3 days on average. The longest period of time without a step occurring was 5.08 days. To examine these step features more closely, we analyzed the spectra from one of these events. We found that the integral of the spectra rose from 8833 ± 93.98 to 17190 ± 131.11 during the event, a increase of 194.6%.

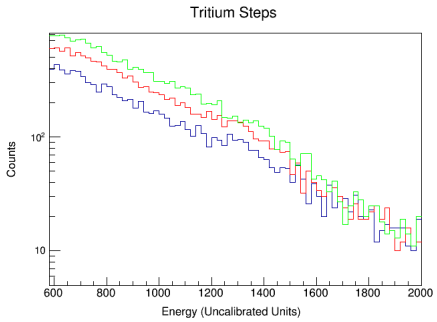

Figure 10: An overlay of three spectra from a step in CH_3T after bypassing our purifier. The blue spectrum was collected prior to a step occurring, the red spectrum was collected while a step was occurring, and the green spectrum was collected after the step had reached a plateau.

Such an increase in CH_3T activity can be produced through two mechanisms – a drift in PMT gain which would shift the CH_3T spectrum horizontally, or an increase in CH_3T activity shifting the CH_3T spectrum vertically. To determine if our PMT gain was shifting during our CH_3T data sets we used an external Cesium-137 to a construct time histogram of the Cesium-137 rate. Over eight days the Cesium-137 event rate remained flat, with an initial event rate of 120255 ± 346.778 (observed Bq) and a final event rate of 115469 ± 339.807 (observed Bq). We conclude that the rise in tritium rate during the step events can not be due to our PMT gain drifting, and

must therefore be a result of an increase in the amount of CH_3T in the fiducial region of our detector. We suspect this increase in CH_3T is due to pockets of stagnant gas slowly moving into the detector's fiducial region. To avoid such a source of residual CH_3T contamination, a detector wishing to using tritiated methane as an internal calibration source must be designed such that no areas of stagnant gas exist within its system.

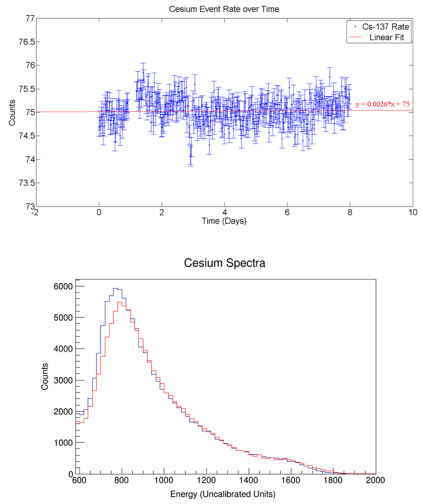

Figure 11: Top: A time histogram of Cesium-137 events in our detector. Bottom: An overlay of the initial and final Cs-137 spectrum from above.

We can fit the integral of our equation for the flux out of the plastic over time to the outgassing data collected in Maryland's liquid xenon system to extract a value for the constant G. Since these outgassing data includes step features from stagnant pockets of unpurified CH_3T, we can set an upper limit on G by assuming the step features are a result of outgassing itself, and a lower limit on G by subtracting the steps out of our data, treating them as if they have no connection to outgassing at all. With this method we loosely constrain $0.001 \frac{cm}{\sqrt{day}} \leq G \leq 0.01 \frac{cm}{\sqrt{day}}$.

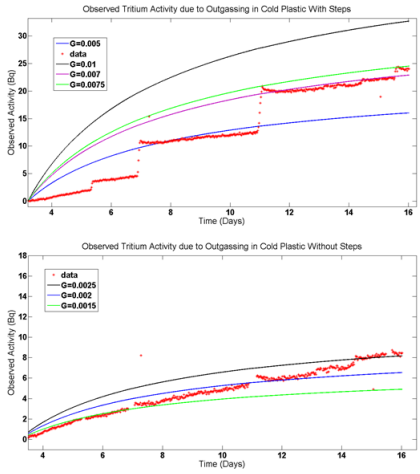

Figure 12: Top: A fit of the integral of the flux of CH_3T out of plastic over time assuming that the step features are due to diffusion. This fit is used to set an upper limit on G. Bottom: A fit of the integral of the flux of CH_3T out of plastic over time assuming that the step features are not due to diffusion. This fit is used to set a lower limit on G.

B. Implications for LUX

With a constraint on G taken from the analytic solution to Fick's second law, we turn to numerical simulation to answer the question of how much initial CH_3T activity to inject into LUX to meet our

calibration conditions. Several assumptions are made to simplify the numerical model. First, we approximate the diffusion into plastic as being a one dimensional process. In three dimensions, Fick's laws are

$$J = -D\nabla\phi$$

$$\frac{\delta\phi}{\delta t} = D\nabla^2\phi.$$

In cylindrical coordinates, these equations become

$$J = -D(\frac{\delta\phi}{\delta r}\vec{r} + \frac{1}{r}\frac{\delta\phi}{\delta\theta}\vec{\theta} + \frac{\delta\phi}{\delta z}\vec{z})$$

$$\frac{\delta\phi}{\delta t} = D(\frac{\delta^2\phi}{\delta r^2} + \frac{1}{r}\frac{\delta\phi}{\delta r} + \frac{1}{r^2}\frac{\delta^2\phi}{\delta\theta^2} + \frac{\delta^2\theta}{\delta z^2}).$$

Since the plastic in our detector at Maryland and in LUX can be approximated by a cylindrical shell, there is no dependence on the azimuthal or z coordinates. Since r is large compared to the thickness of the plastic shell, $\frac{\delta^2\phi}{\delta r^2} \gg \frac{1}{r}\frac{\delta\phi}{\delta r}$, so we can make the approximations

$$J = -D\frac{\delta\phi}{\delta r}\vec{r}$$

$$\frac{\delta\phi}{\delta t} = D\frac{\delta^2\phi}{\delta r^2}.$$

We assume the concentration of CH_3T in LUX is uniform throughout its volume. This assumption is justified, since the design of LUX creates currents which stir the liquid xenon. With perfect mixing the effect of the purifier can be modeled by adding an exponential time dependence to the outer volume. The time constant of this decay is equal to the time it takes xenon to recircculate through the LUX detector.

We use a simple implementation of the first order Euler method for our numerical simulations. The finite difference approximations of Fick's two laws in one dimension are

$$J_{i,j} = -D\frac{\phi_{i+1,j} - \phi_{i,j}}{\Delta x}$$

$$\phi_{i,j+1} = \phi_{i,j} + \Delta t(D\frac{\phi_{i+1,j} - 2\phi_{i,j} + \phi_{i-1,j}}{\Delta x^2}),$$

where i is the spacial index and j is the time index. To avoid divergent solutions, we must have

$$D\frac{\Delta t}{\Delta x^2} \leq \frac{1}{2}.$$

For effects to be propagated across N spacial bins, N time steps are required. Therefore, the effective time resolution is

$$\Delta t_{effective} = \Delta t \times N_x.$$

The diffusion is simulated by setting the concentration at the boundary of the piece equal to KC_{out}, where C_{out} is the concentration of CH_3T in the xenon. This concentration is dependent on time according to

$$\frac{\delta C_{out}}{\delta t} = J_{out}\frac{A_{plastic}}{V_{xenon}} - \frac{C_{out}}{\tau},$$

where $A_{plastic}$ is the surface area of the plastic cylinder, V_{xenon} is the total volume of xenon in the fiducial region, and τ is the time it takes for one full purification cycle. The first term on the

right of this equation models outgassing of CH_3T from the plastic cylinder, while the second term models removal of CH_3T through purification. Using the first order Euler method, we arrive at an expression for C_{out} given by

$$C_{j+1} = C_j + \Delta t[(J_{1,j} - J_{N_x,j})\frac{A_{plastic}}{V_{xenon}} - \frac{C_j}{\tau}].$$

The initial concentration is defined by dividing the desired injection activity by the volume of the fiducial region. We choose $D = 2.3 \times 10^{-9} \frac{cm^2}{sec}$ such that the half-infinite boundary conditions in our diffusion model is valid, and combine this with our allowed range of values for G to extract a value for K. We find that for all G values in our allowed range, an initial injection activity of 0.1 Bq results in 15,000 calibration events with the background rate returning to $< 5\%$ of its initial value in less than one month.

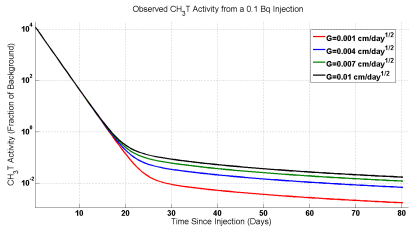

Figure 13: Simulated activity over time in LUX after a 0.1 Bq injection.

NOTE: UPDATE THIS SECTION, REDO EVERYTHING WITH SAME FIDUCIAL VOLUMES, TIME CONSTANTS, ETC

IV. Experimental Setup

The setup of our triated methane calibration technique can be separated into three parts: the injection system, the tritiated methane source bottle, and the zirconium getter.

A. The tritiated methane source

The tritiated methane source bottle for our calibration technique consists of a 2250 cc stainless steel bottle which is filled with a mixture of tritiated methane and xenon. This source bottle was prepared in three steps. First, we prepared a xenon bottle that had similar pressure and purity to the LUX system. We filled a 2250 cc stainless steel bottle with 1590 torr of xenon from the same dekryptonation and purity program which the LUX xenon came from. The purpose of this xenon was to serve as a carrier gas for the triaited methane. The next step was to prepare a small amount of tritiated methane to mix with this dekryptonated xenon. A reservoir of tritiated methane with an activity of 204 Bq/torr-cc was purchased from Moravek Biochemical. The reservoir was frozen with liquid nitrogen, resulting in a vapor pressure of 10.4 $\pm$ 0.05 torr. We then opened the frozen tritiated methane reservoir to a 1/4" VCR cross which was sealed with swagelok valves on each side. This first expansion space had a total volume of 5.2 $\pm$ 0.9 cc. Next, we isolated the VCR cross from the triated methane reservoir and then opened it to a 501 $\pm$ 0.2 cc expan-

sion volume. We isolated the VCR cross a second time and then opened it up to a 53.2 ± 3.4 cc expansion volume. The VCR cross was then isolated for a third time before opening it to a 10.5 ± 0.5 cc expansion volume. After this final expansion the VCR cross was isolated and the remaining 0.016 ± 0.006 torr-cc of tritiated methane left within was mixed with the dekryptonated xenon inside the 2250 cc bottle via cryopumping. The final result was a tritiated methane source which had an activity of 9.1e-7 ± 3.4e-7 Bq/torr-cc.

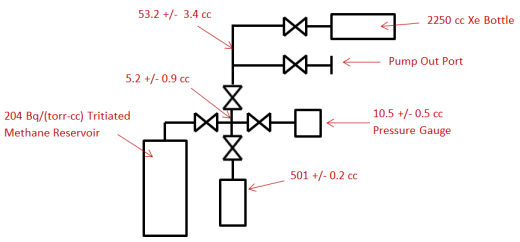

Figure 14: The volume sharing system that was built to assemble our tritiated methane source bottle.

B. The injection system

The injection system for our tritiated methane calibration technique consists of a series of expansion volumes which are used to fine tune the amount of CH_3T that is injected. Once the CH_3T source bottle is opened it flows through a methane gas purifier (SAES MC1-905F) to remove any sources of potential contamination, such as bare tritium. The CH_3T then flows into the expansions volumes set by the user. We use expansion volumes of 9.8 ± 0.4 cc , 13.3 ± 0.4 cc, 26.0 ± 0.5 cc, 82.7 ± 0.5 cc, 120.0 $/pm$ 0.6 cc, and 132.7 ± 0.6 cc in our experimental setup, giving us a range of 0.014 ± 0.005 - 0.556 ± 0.208 Bq. Once the expansion volumes have filled, the flow of xenon in the gas system is diverted through the expansion volumes to sweep the CH_3T into the detector. We continue to flow through the expansion volumes for one hour, which is equivalent to flushing out the expansion volumes over 1000 times, since LUX flows at 20 SLPM and the full 384.5 cc of the expansion volumes are filled with 1590 torr of the xenon and CH_3T mixture. A pump out port allows the expansion volumes to be evacuated in preparation for each use of the injection system. Note that each injection will lower the total activity in the CH_3T source bottle via volume sharing, results in a smaller, yet calculable, injection activity with subsequent injections. A pressure gauge (PT-T1) is included above the tritiated methane source bottle so that this drop in activity can be measured. The final component of the injection system is a particle filter (Mott Corp. GSP3752FF11) which prevents particles contaminants from entering the detector.

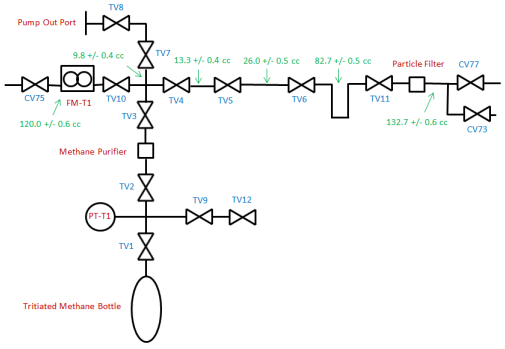

Figure 15: The injection system used in our CH_3T calibration technique. CV and TV labels indicate valves in the LUX circulation system and tritium injection system, respectively. Expansion volumes are labeled in green, and other system components are labeled in red.

C. The zirconium getter

The LUX gas system uses a hot zirconium getter (SAES-PS4MT15R1) downstream of the CH_3T injection system to remove CH_3T from the xenon. Extensive R&D was conducted using a smaller zirconium getter (SAES-PF4C3R1) at the University of Maryland to learn about the CH_3T removal efficiency of these purifiers. Details of these studies is discussed in section II.

V. Injection Strategy

The LUX collaboration agreed upon a three phase plan for a safe and successful tritium injection. The first phase of this plan was a natural methane injection using the tritiated methane injection system for the purpose of determining the purification time constant in LUX. The second phase of the plan was a small tritium injection (19 mBq) into LUX. This small injection would highlight any potential problems before injecting a larger amount of tritium, and it would determine if any scaling factor was needed between the absolute injection activity and the observed injection activity. Additionally, the small tritium injection would allow us to measure the fraction of tritium that goes into the fiducial volume. Finally, the third phase of the plan was to use what we learned from the first two phases to safely inject a larger amount of tritium (15,000 events) for the purpose of measuring the ER rejection factor of LUX and cross-checking the NEST prediction of the ER band.

NOTE: SHOULD I PUT 19 mBq as the target, or adjust it now that we know the factor of 2 issue? The number of events and the target rate are not what we actually got, but we know this is due to the volume measurements being off.

A. Phase One

During phase one 0.02 grams of natural methane were injected into LUX using the tritium injection system. Purity samples from the detector were collected over the next few days, and a purification time constant of 5.90 ± 0.07 hours was determined using data collected with the LUX gas sampling system.

NOTE: ASK JON FOR EXACT METHANE AMOUNT

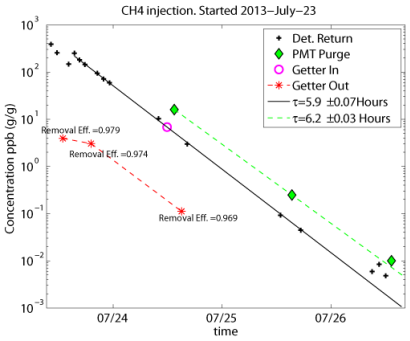

Figure 16: First three days of the natural methane injection. The discontinuity near the beginning of the data is due to a secondary natural methane injection.

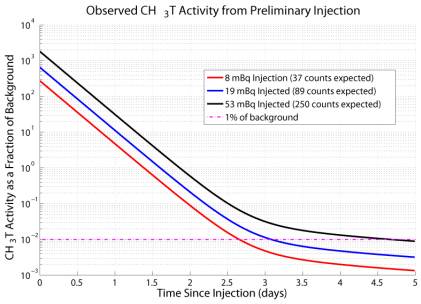

Figure 17: Simulation of various tritium injections into LUX.

B. Phase Two

During phase two ?? ± ?? mBq of CH_3T was injected into LUX. The simulations which are discussed in section ?? predicted that we should see ?? events in the fiducial volume given a ?? mBq injection, a six hour purification time constant, and an immediate removal of 20% of the injected activity by the purifier. The immediate removal of 20% of the injected activity was motivated by what we have seen during the natural methane injection into LUX. These simulations assumed that the remaining 80% of the activity would go into the liquid xenon in the detector, and that the fiducial fraction would be $\frac{100}{375} = 26.6\%$.

The first 23 hours of data show that the initial injection activity in the fiducial volume was 24.2 ± 0.3 mBq, while the initial injection activity in the entire detector was 44.9 ± 0.5 mBq. For this analysis we define the fiducial region as being 30 to 320 μs in Z = 45cm. (1.55 mm/μs drift), with r < 17.5 cm. The activity fell with a purification time constant of 6.9 ± 0.4 hours within the fiducial volume, and a purification time constant of 7.7 ± 0.4 hours in the entire detector.

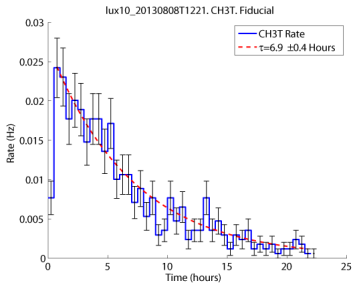

Figure 18: Event rate in fiducial region after the smaller tritium injection into LUX.

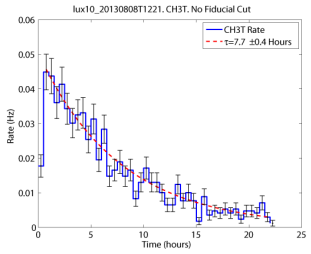

Figure 19: Event rate in entire detector after the smaller tritium injection into LUX.

NOTE: UPDATE THESE PLOTS, ESPECIALLY THE SIMULATION PLOT. CHANGE FIDUCIAL FRACTION IN SIMS TO MATCH DATA ANALYSIS

C. Phase Three

During phase three ?? ± ?? mBq was injected into LUX. The simulations which are discussed in section ?? predicted that we should see ?? events in the fiducial volume given a ?? mBq injection, a six hour purification time constant, and an immediate removal of 20% of the injected activity by the purifier. The immediate removal of 20% of the injected activity was motivated by what we have seen during the natural methane injection into LUX. These simulations assumed that the remaining 80% of the activity would go into the liquid xenon in the detector, and that the fiducial fraction would be $\frac{100}{375} = 26.6\%$.

NOTE: MAKE PLOT OF SIMULATIONS FOR THIS SET UP

The first ?? hours of data show that the initial injection activity in the fiducial volume was ?? ± ?? mBq, while the initial injection activity in the entire detector was ?? ± ?? mBq. For this analysis we define the fiducial region as being ?? to ?? μs in Z = ??cm. (1.55 mm/μs drift), with r < ?? cm. The activity fell with a purification time constant of ?? ± ?? hours within the fiducial volume, and a purification time constant of ?? ± ?? hours in the entire detector.

NOTE: MAKE PLOTS OF RATES IN FID AND NON FID

VI. Results

LUX's NEST simulations closely predicted the electron recoil band. In the first ?? hours of data there were ?? ± ?? events inside of the predicted ER band out of a total of ?? ± ?? events in the fiducial region. Thus, the 90% confidence bands constructed by NEST contained ??% ± ??% of the tritium events.

NOTE: MAKE NEST PLOTS FOR FID

The mass of xenon in the fiducial volume is 125 kg, while the entire mass of liquid xenon seen by the PMTs is 285 kg. The total number of tritium events seen in the first ?? hours within the fiducial volume is ?? ± ??, while the total number of tritium events seen in the first ?? hours in the entire detector is ?? ± 32.4. Since the event ratio in the fiducial volume compared to the total volume is ?? ± ??, and the mass ratio of the fiducial volume to the total volume is ??, the tri-

tium events appear to be fairly uniform throughout the detector.

The event rate in the LUX detector returned to the initial background rate of ?? ± ?? Hz after ?? days. A comparison of events in the fiducial region before and after the CH_3T calibration shows the complete removal of the CH_3T source.

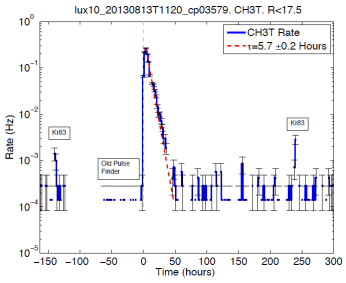

Figure 20: A time histogram of the ?? Bq CH_3T injection into LUX.

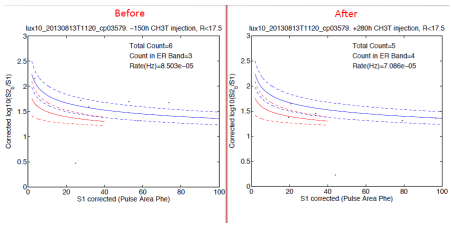

Figure 21: Events in the fiducial region of LUX before and after the CH_3T calibration.

NOTE: MAKE DISTRIBUTION AND SPREAD PLOTS NOTE: MAKE PLOTS AND REDO NUMBERS AFTER DATA HAS BEEN REPROCESSED

VII. Summary

We have presented our new technique for injecting and removing CH_3T as an internal calibration source in detectors which utilize liquid and gas phase noble gases. We discussed the assembly of our CH_3T calibration system, motivated by gas and liquid phase R&D experiments at the University of Maryland. We have used data from the LUX detector to show that our system can safely inject CH_3T for the purpose of internal calibration.

References

[1] McKinsey, et al. *Journal of Physics: Conference Series* 203:012026 (2010)

[2] Fiorucci, et al. *AIP Conference Proceedings* 1200:977 (2010)

[3] Kastens, et al. *Phys. Rev. C* 80:045809 (2009)

[4] Miyake, et al. *J. vac. Sci. technol. A.* 1:1446-1451 (1983)

[5] R. Piche. *Partial Differential Equations* Tampere University of Technology.